Advanced Aerodynamic Analysis of the NASA High-Lift Trap Wing with a Moving Flap Configuration

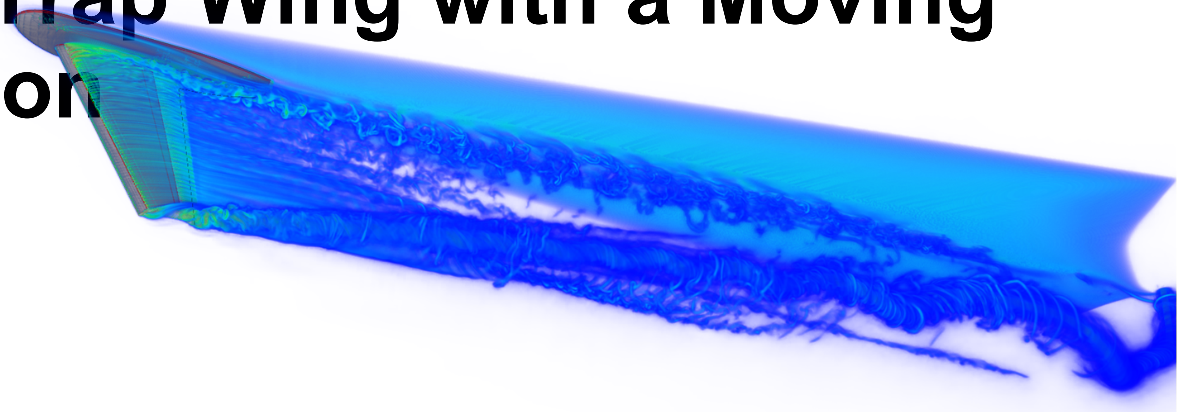

David M. Holman

Outline

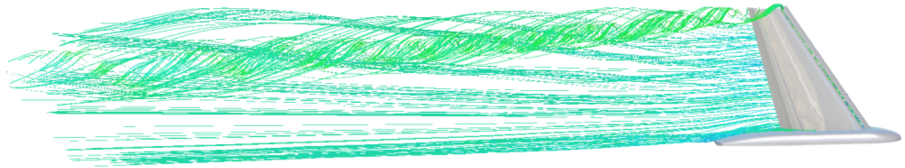

- **Introduction**
- Numerical Methodology
- 1st High Lift Prediction Workshop Results
- Polar Sweep
- Stowing and Un-Stowing
- Summary

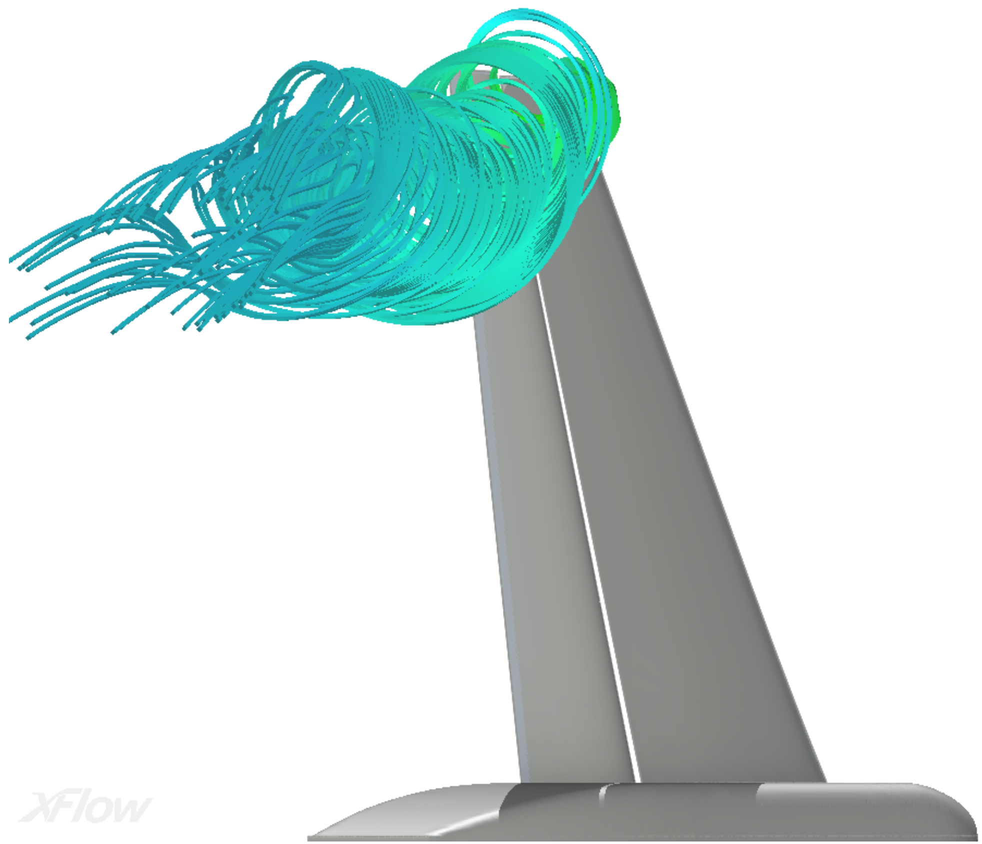

Introduction

XFlow is a CFD software specifically designed to simulate complex systems involving highly transient flows and even the presence of moving parts

These two areas have traditionally proven to be difficult to treat with classic FEM/FVM schemes

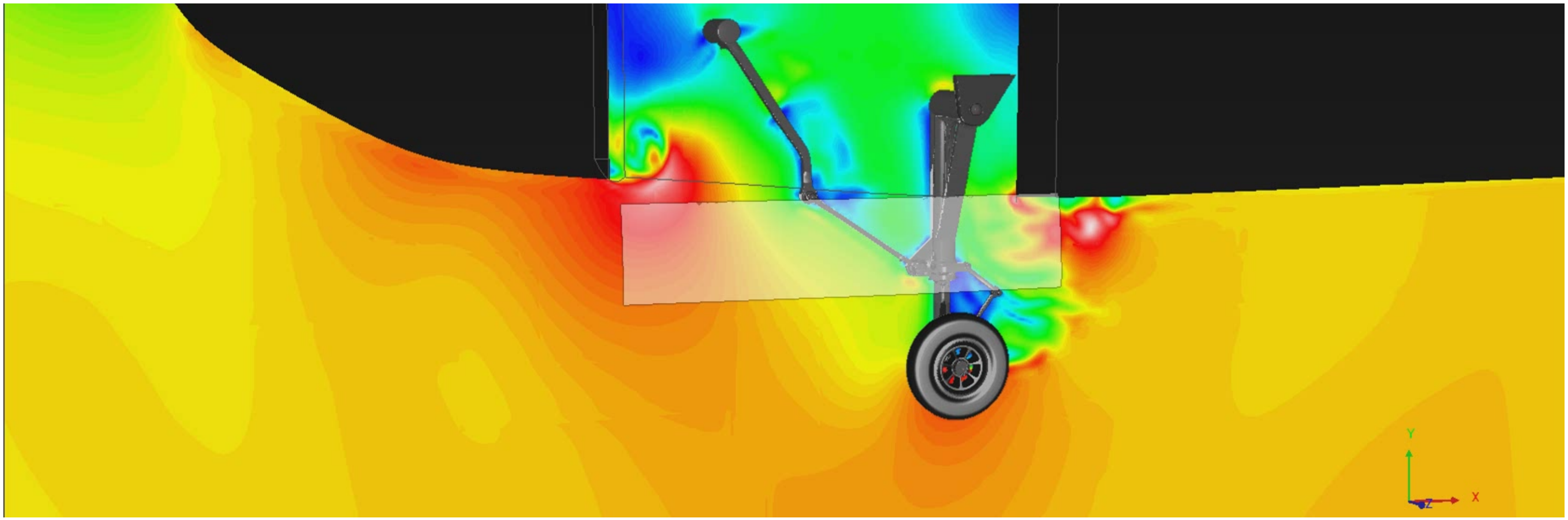

Introduction

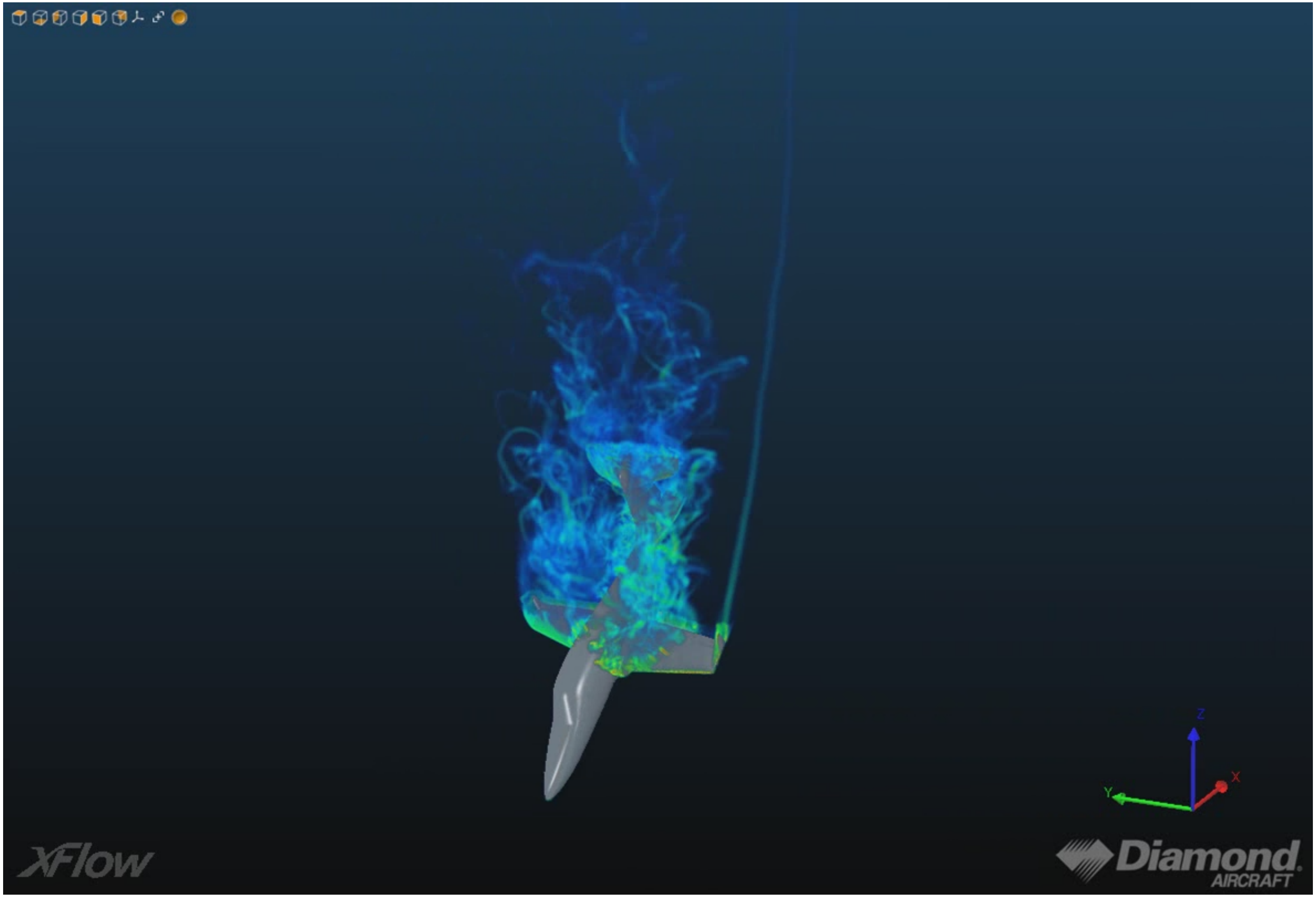

Numerical methodology

Over the last few years schemes based on minimal kinetic models for the Boltzmann equation are becoming increasingly popular as a reliable alternative over conventional CFD techniques

LGA

$$n_i(\mathbf{r}+\mathbf{e_i}, t+dt) = n_i(\mathbf{r}, t) + \Omega_i(n_1, ..., n_b)$$

$$\rho = \frac{1}{b}\sum_{i=1}^{b} n_i$$

$$\rho\mathbf{v} = \frac{1}{b}\sum_{i=1}^{b} n_i\mathbf{e}_i$$

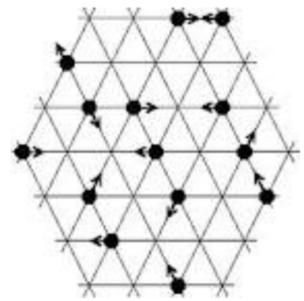

LBM

$$\frac{\partial f_i}{\partial t} + \mathbf{e}_i \cdot \nabla f_i = \Omega_i,\ i = 1, ..., b$$

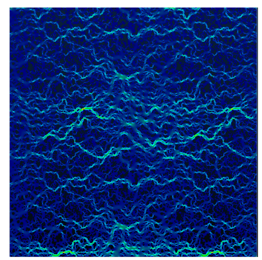

Numerical methodology

The collision operator in XFlow is based on a multiple relaxation time scheme

SRT

$$\Omega_i^{\mathrm{BGK}} = \frac{1}{\tau}(f_i^{\mathrm{eq}} - f_i)$$

MRT

$$\Omega_i^{\mathrm{MRT}} = M_{ij}^{-1}\hat{S}_{ij}(m_i^{\mathrm{eq}} - m_i)$$

Numerical methodology

As opposed to standard MRT, the scattering operator is implemented in central moment space.

SRT

$$\Omega_i^{\mathrm{BGK}} = \frac{1}{\tau}(f_i^{\mathrm{eq}} - f_i)$$

MRT

$$\Omega_i^{\mathrm{MRT}} = M_{ij}^{-1}\hat{S}_{ij}(m_i^{\mathrm{eq}} - m_i)$$

Raw moments

$$\mu x^k y^l z^m = \sum_i^N f_i e_{ix}^k e_{iy}^l e_{iz}^m$$

Central moments

$$\tilde{\mu} x^k y^l z^m = \sum_i^N f_i (e_{ix} - u_x)^k (e_{iy} - u_y)^l (e_{iz} - u_z)^m$$

Numerical methodology

The approach used for turbulence modeling is the WMLES

The Wall-Adapting Local Eddy viscosity model provides a consistent local eddy-viscosity and near wall behavior

$$
\begin{aligned}
\nu_t &= \Delta_{\mathrm{f}}^2 \frac{(G^d_{\alpha\beta} G^d_{\alpha\beta})^{3/2}}{(S_{\alpha\beta} S_{\alpha\beta})^{5/2} + (G^d_{\alpha\beta} G^d_{\alpha\beta})^{5/4}} \\
S_{\alpha\beta} &= \frac{g_{\alpha\beta} + g_{\beta\alpha}}{2} \\
G^d_{\alpha\beta} &= \frac{1}{2}(g^2_{\alpha\beta} + g^2_{\beta\alpha}) - \frac{1}{3}\delta_{\alpha\beta} g^2_{\gamma\gamma} \\
g_{\alpha\beta} &= \frac{\partial u_\alpha}{\partial x_\beta}
\end{aligned}
$$

Numerical methodology

A generalized law of the wall is used to model the boundary layer

$$\begin{aligned}\frac{U}{u_c} &= \frac{U_1+U_2}{u_c} = \frac{u_\tau}{u_c}\frac{U_1}{u_\tau} + \frac{u_p}{u_c}\frac{U_2}{u_p} \\ &= \frac{\tau_w}{\rho u_\tau^2}\frac{u_\tau}{u_c} f_1\left(y^+\frac{u_\tau}{u_c}\right) + \frac{\mathrm{d}p_w/\mathrm{d}x}{|\mathrm{d}p_w/\mathrm{d}x|}\frac{u_p}{u_c} f_2\left(y^+\frac{u_p}{u_c}\right)\end{aligned}$$

$$\begin{aligned} y^+ &= \frac{u_c y}{\nu} \\ u_c &= u_\tau + u_p \\ u_\tau &= \sqrt{|\tau_w|/\rho} \\ u_p &= \left(\frac{\nu}{\rho}\left|\frac{\mathrm{d}p_w}{\mathrm{d}x}\right|\right)^{1/3}. \end{aligned}$$

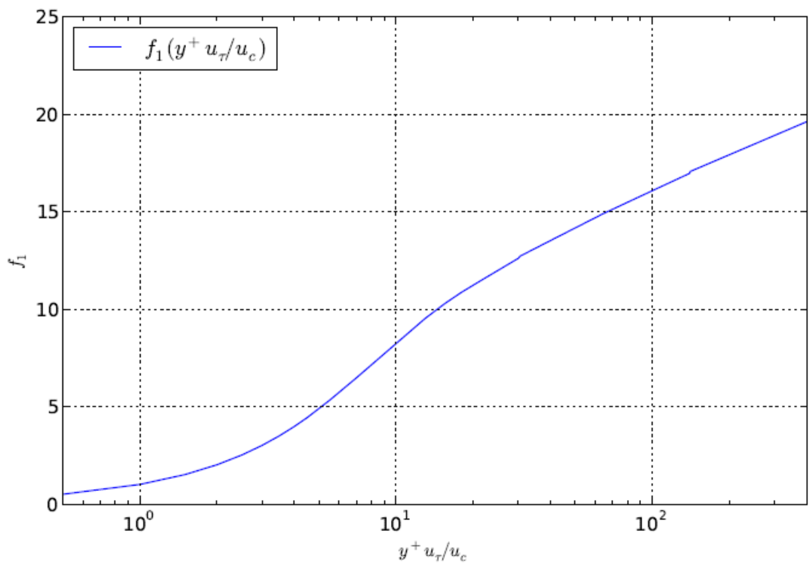

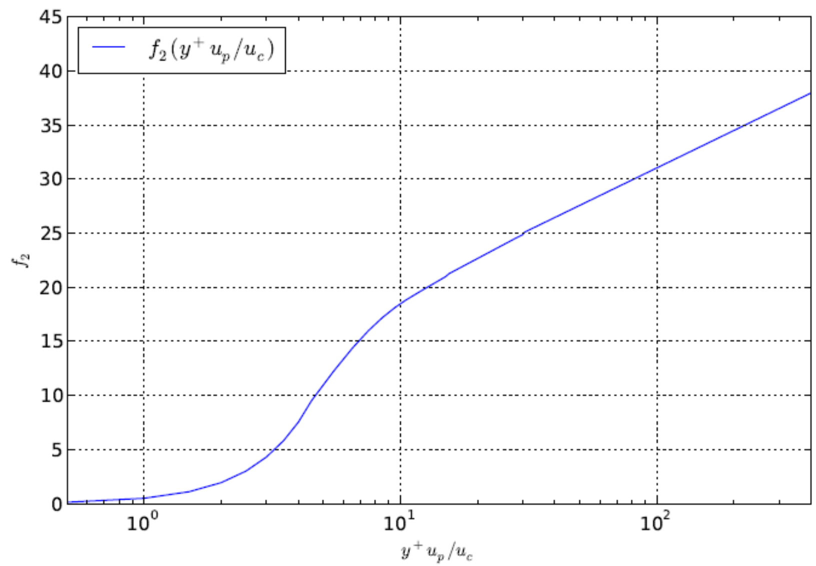

Outline

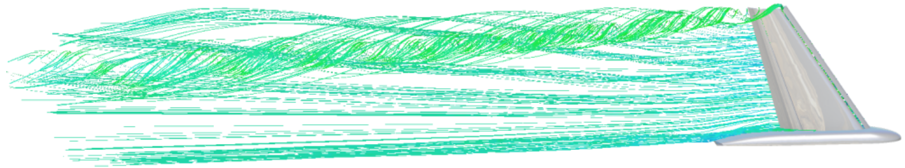

- Introduction
- Numerical Methodology
- **1st High Lift Prediction Workshop Results**
- Polar Sweep
- Stowing and Un-Stowing
- Summary

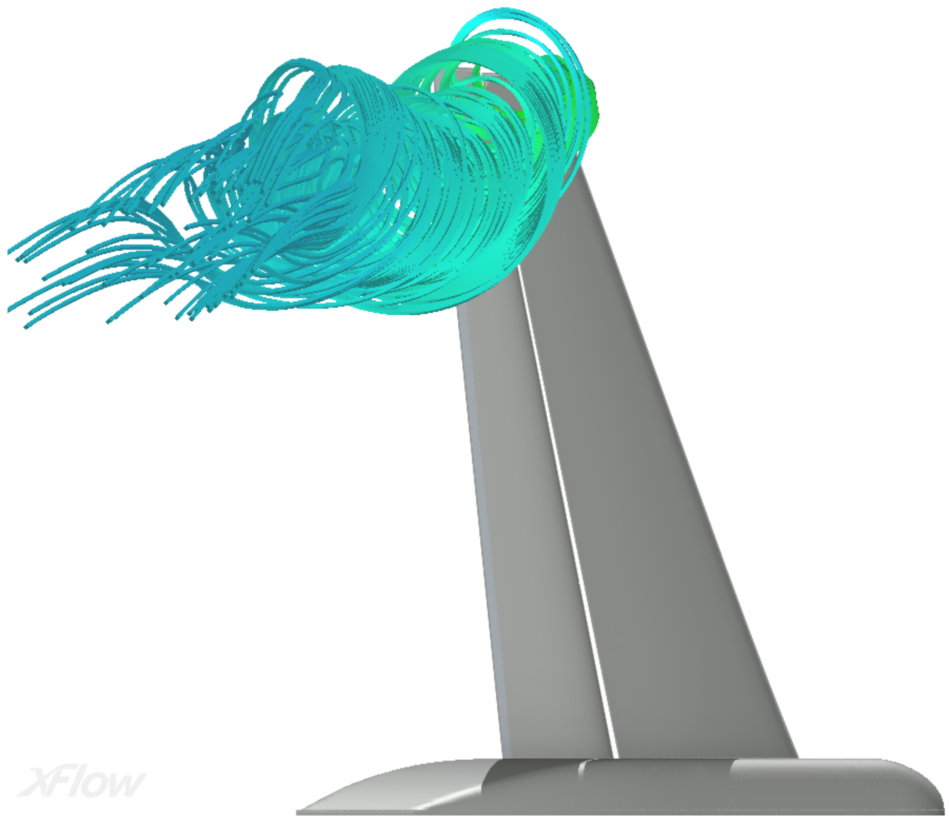

1st High Lift Prediction Workshop Results

- Trap wing "Config 1" (slat 30, flap 25)
- Mach = 0.2
- Reynolds = 4.3E+6 based on MAC
- Mean aerodynamic chord = 1.0067 m
- No brackets
- AoA: -4, 1, 6, 13, 21, 28, 32, 34 and 37 degrees

All the computations were run on a single workstation with two processors Intel Xeon E5620 @ 2.4 GHz (8 cores) and 12GB of RAM

1st High Lift Prediction Workshop Results

Virtual wind tunnel configuration: (40 x 15 x 30) m
Far field velocity as initial boundary condition

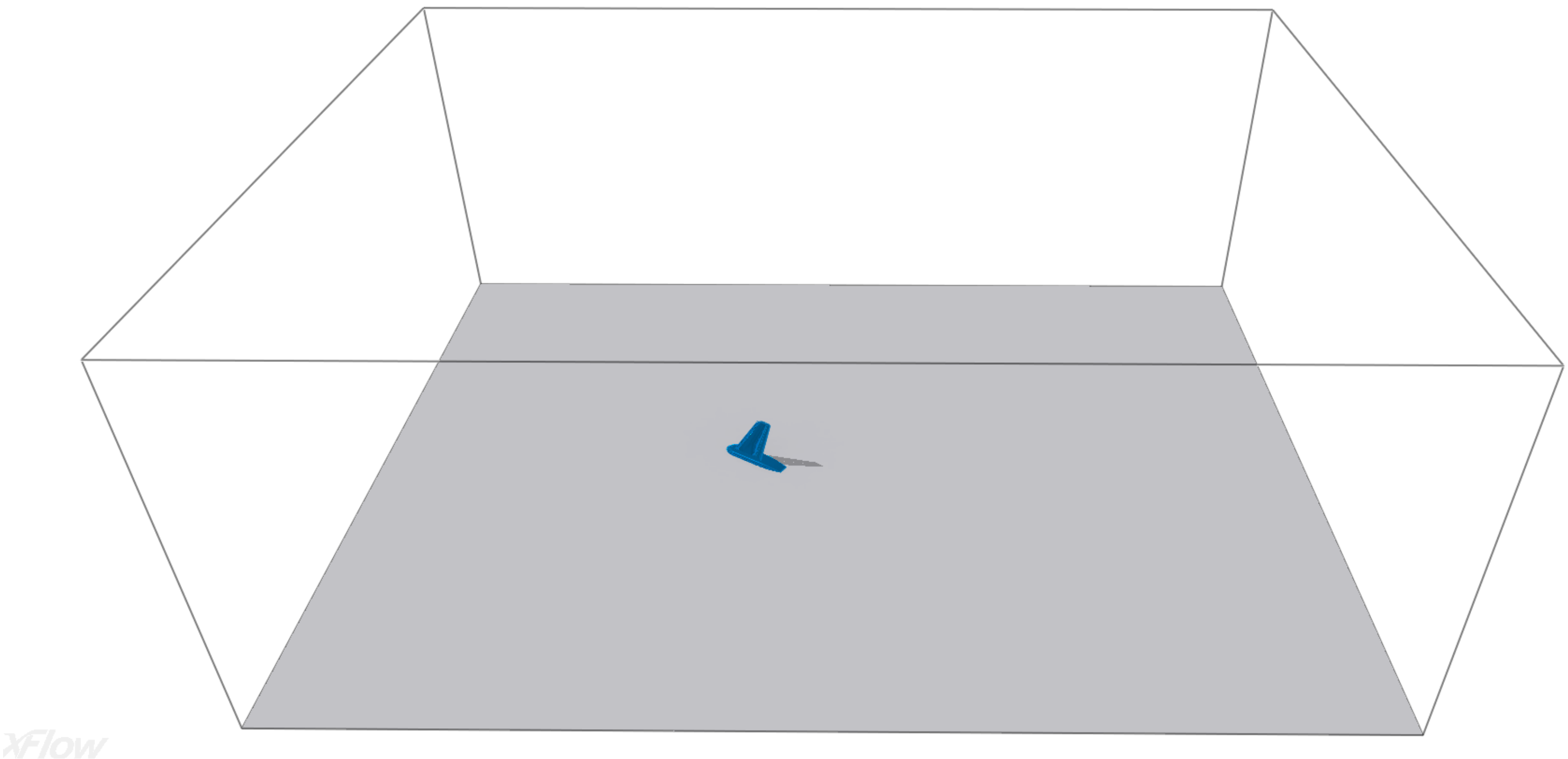

1st High Lift Prediction Workshop Results

Spatial discretization based on adaptive wake refinement

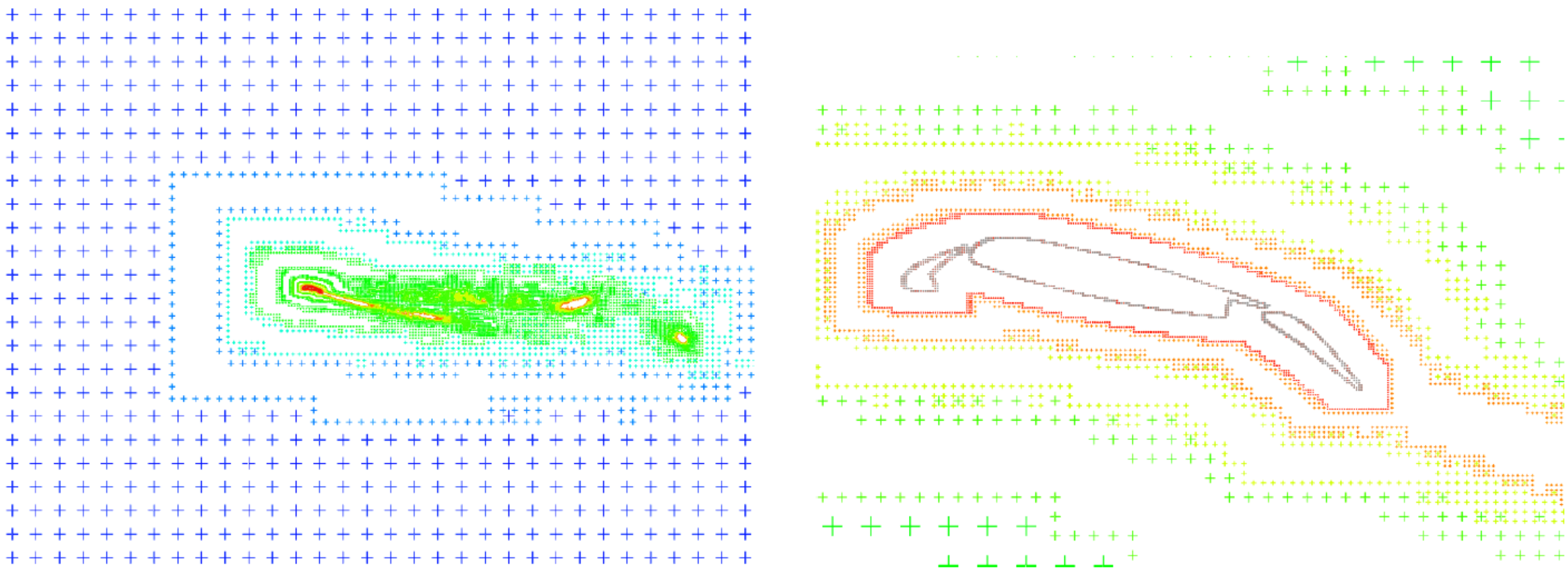

Resolutions used for the resolution-dependency at 13 degrees incidence

	h	$h/2$	$h/2^2$	$h/2^3$
Near wall (m)	0.04	0.02	0.01	0.005
Wake (m)	0.08	0.04	0.02	0.01
# of Elements at $t = 0.3$ s	201,513	653,211	2,893,687	21,880,186

1st High Lift Prediction Workshop Results

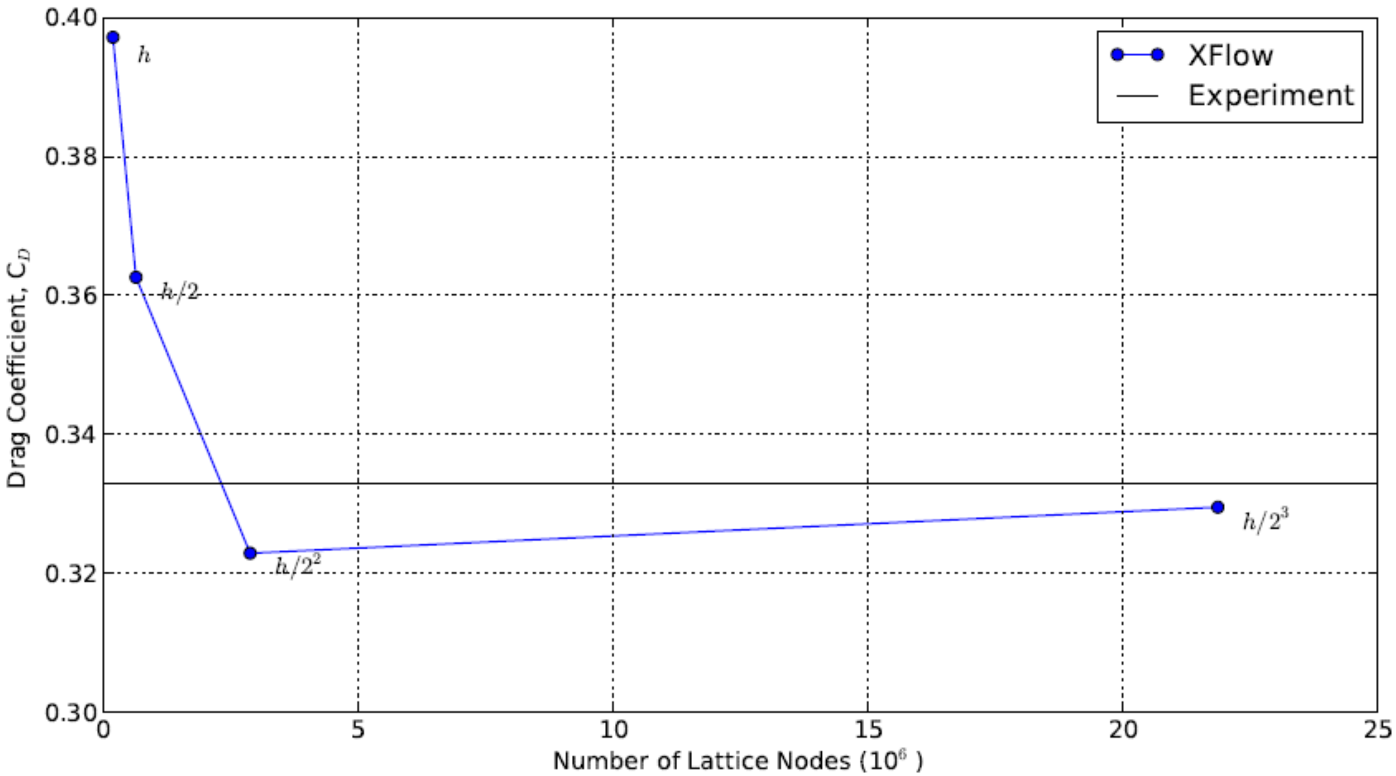

Drag coefficient against the number of lattice nodes for different resolutions at $\alpha = 13°$

1st High Lift Prediction Workshop Results

The resolution is adjusted to keep the maximum number of elements within the memory constrains of a single workstation (12GB)

Resolutions used for the 1^{st} High Lift Prediction Workshop

	Walls (m)	Wake (m)	Far Field (m)	Max. # of Particles	Angles
Resolution 1	0.005	0.01	1.28	25×10^6	[-4°; 32°]
Resolution 2	0.005	0.02	1.28	10×10^6	[34°; 37°]

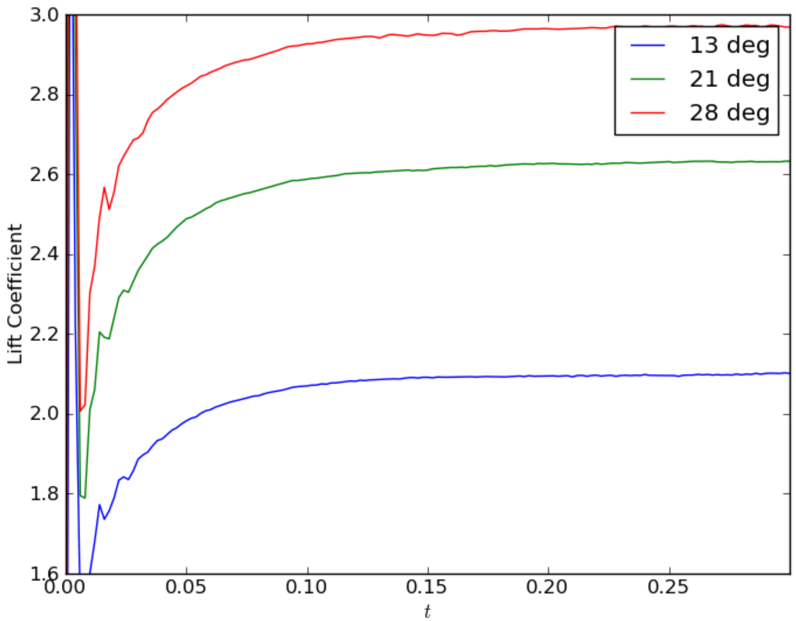

The computation time is 36hours per run using two processors (8 cores)

1st High Lift Prediction Workshop Results

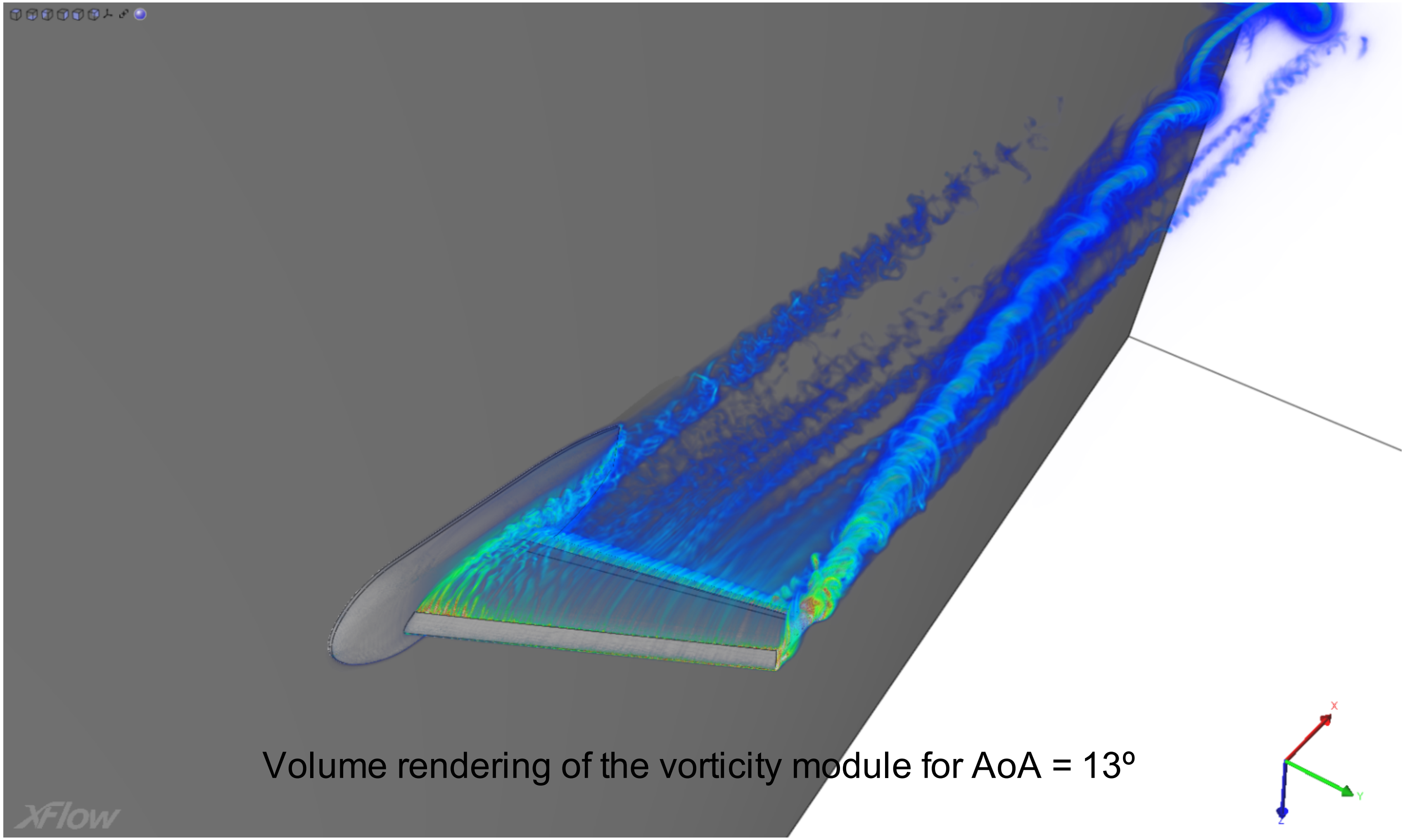

Volume rendering of the vorticity module for AoA = 13º

1st High Lift Prediction Workshop Results

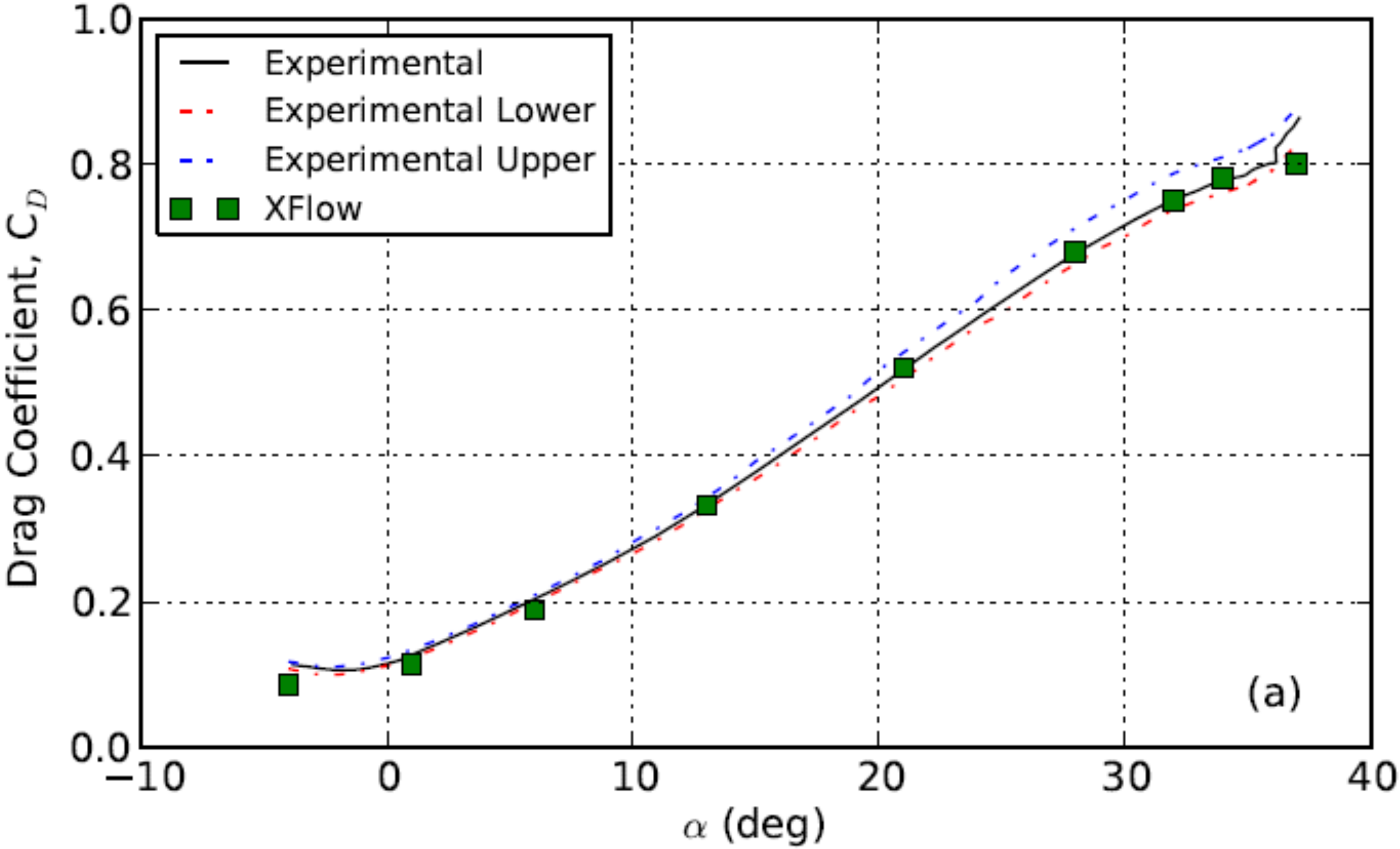

1st High Lift Prediction Workshop Results

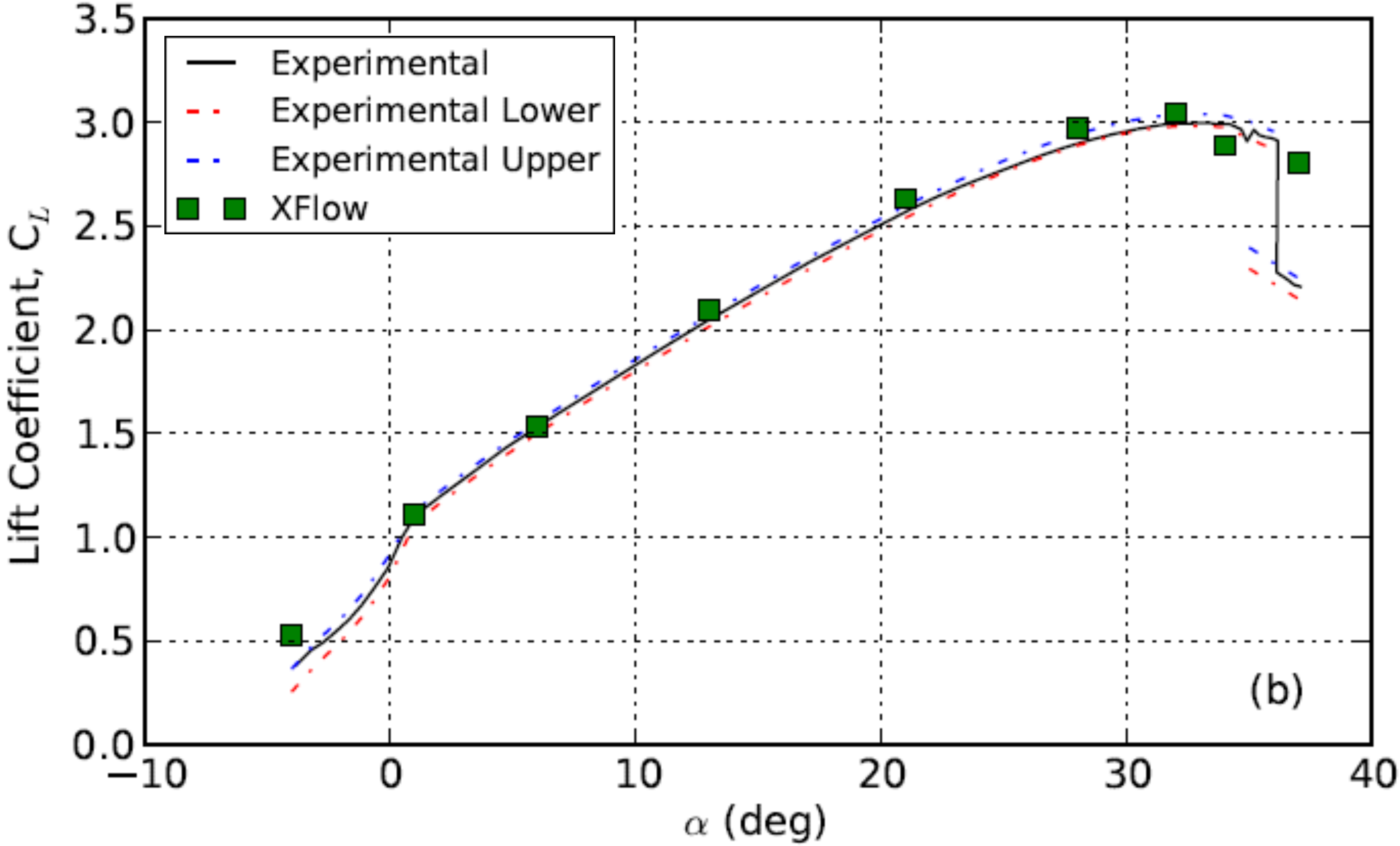

1st High Lift Prediction Workshop Results

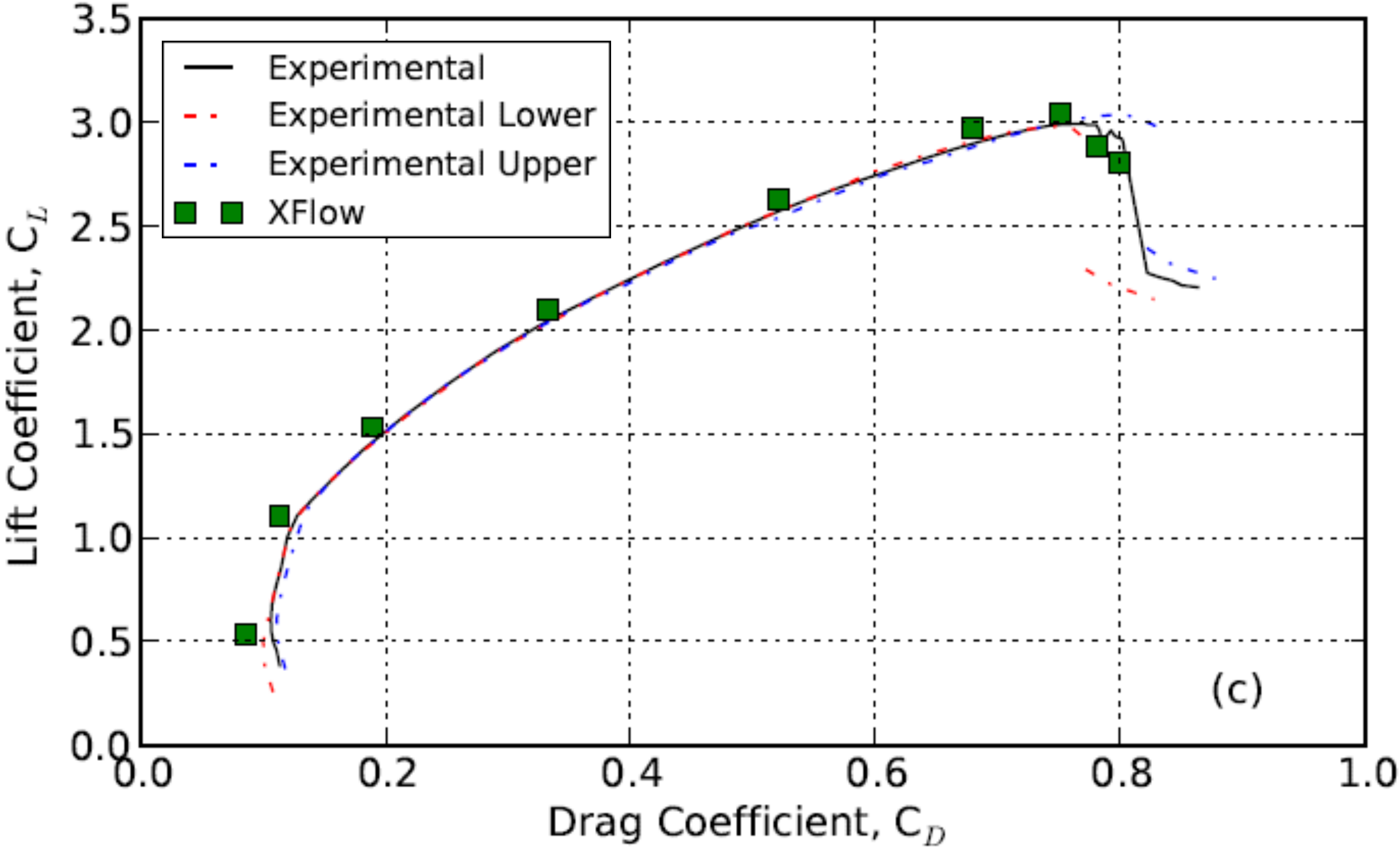

1st High Lift Prediction Workshop Results

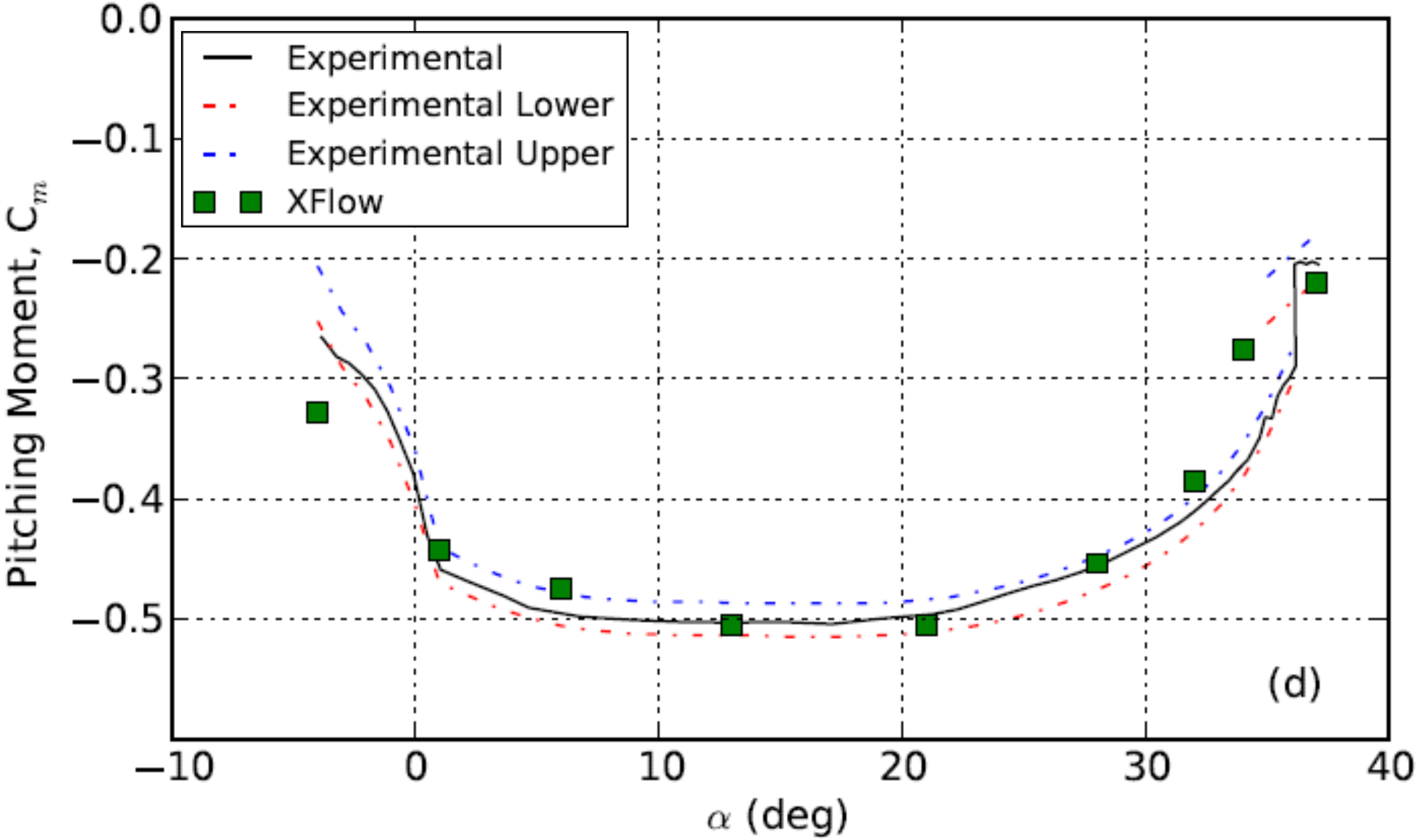

1st High Lift Prediction Workshop Results

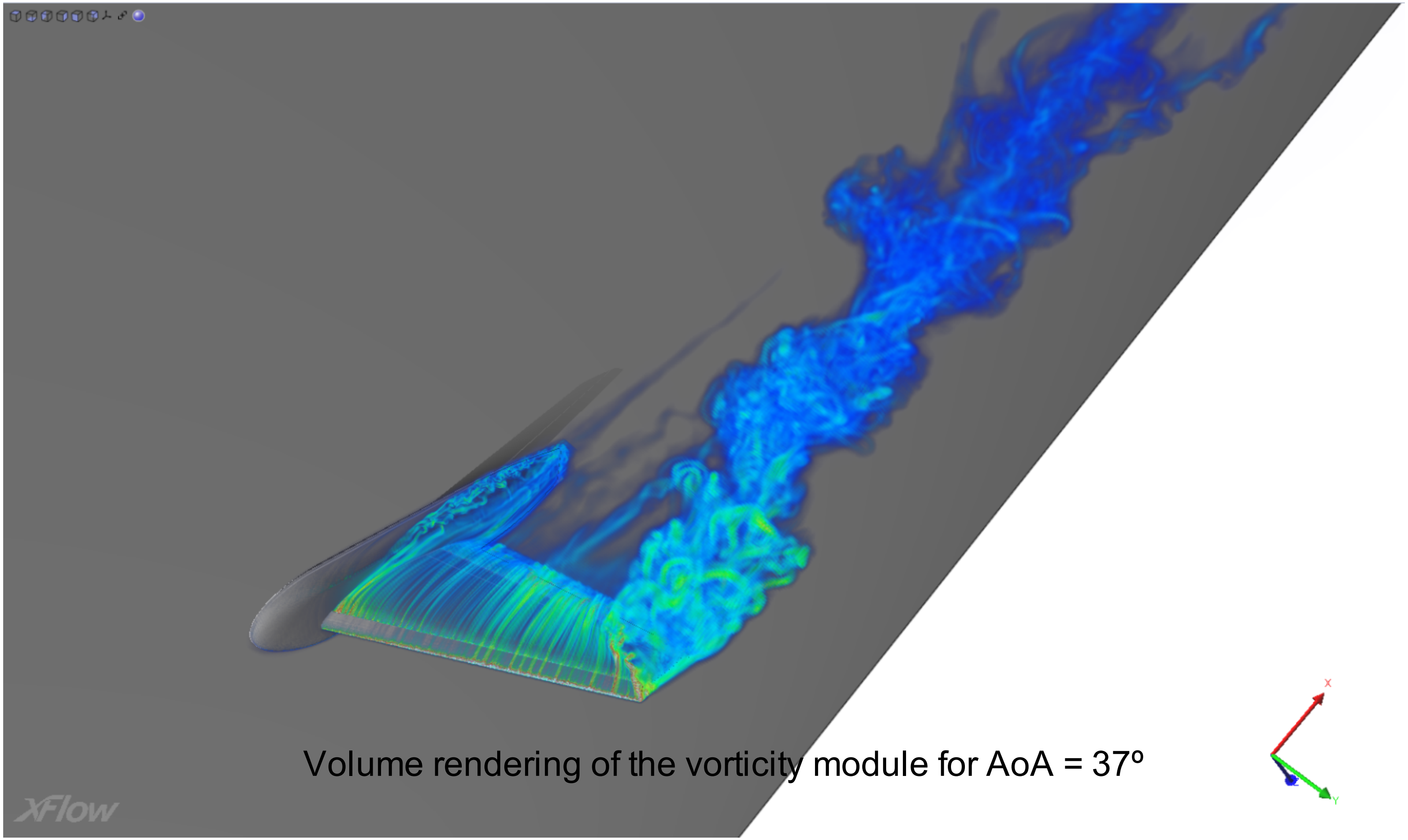

Outline

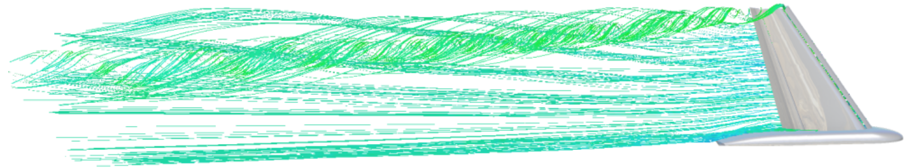

- Introduction
- Numerical Methodology
- 1st High Lift Prediction Workshop Results
- **Polar Sweep**
- Stowing and Un-Stowing
- Summary

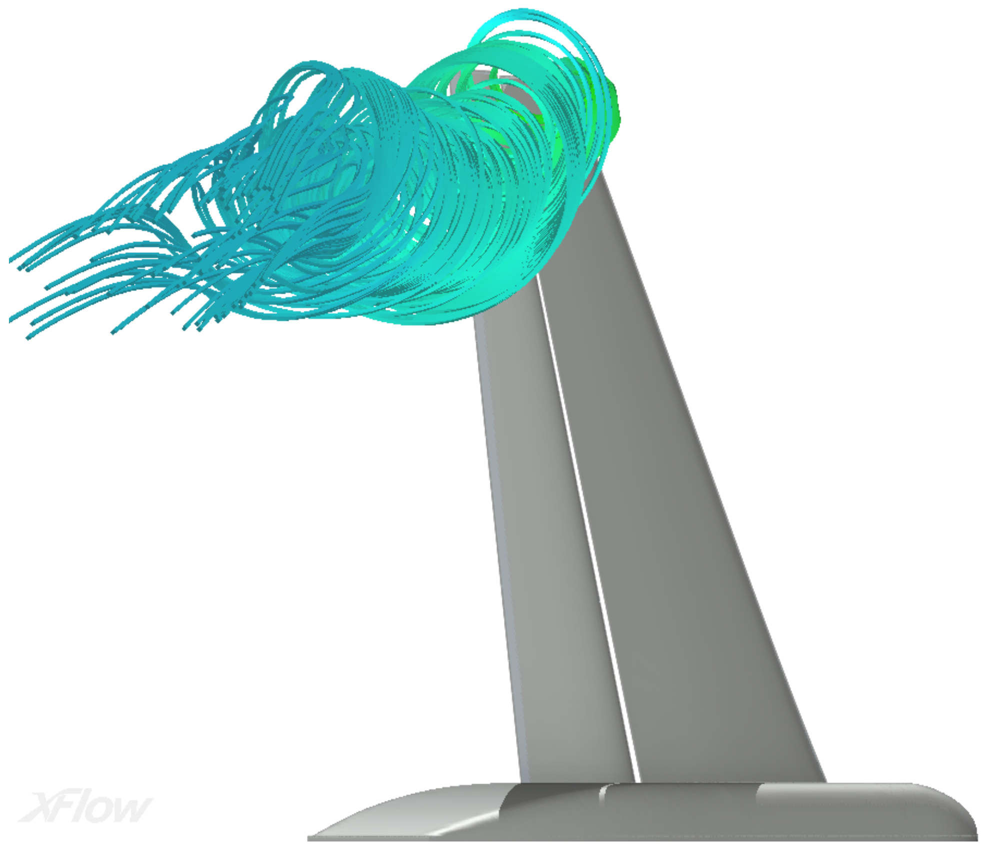

Polar Sweep

Sweep from the linear part of the polar to the stall region

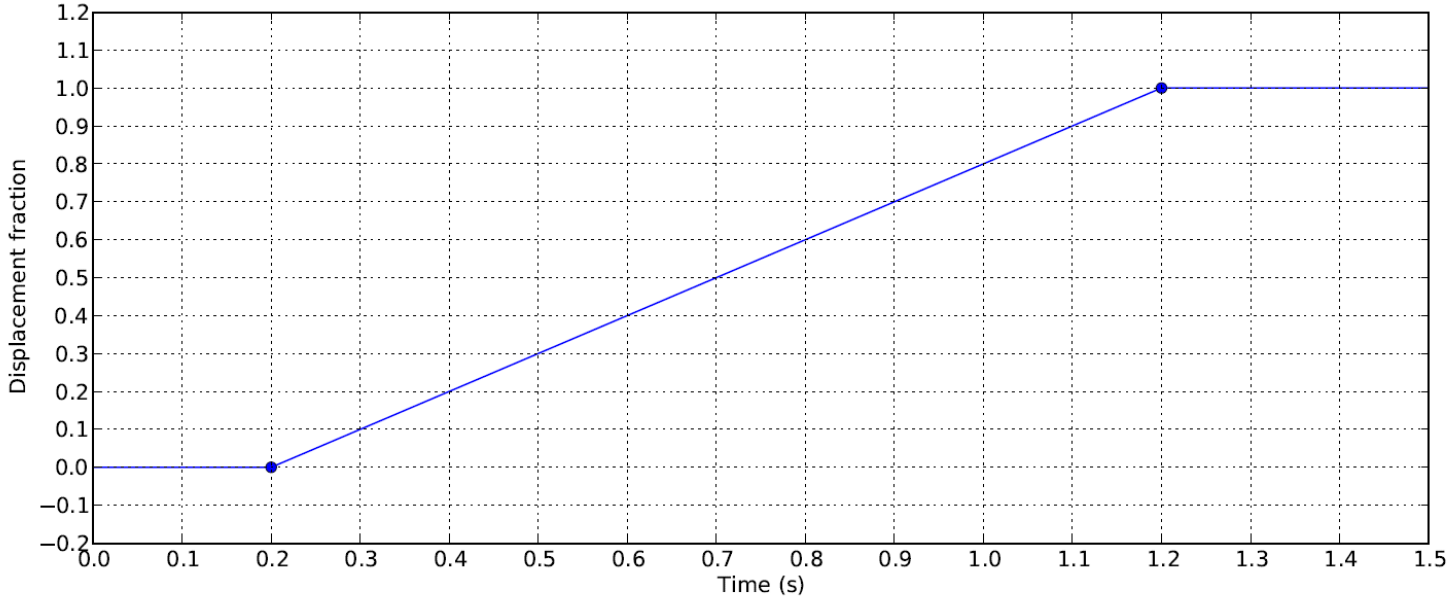

$$v_{\mathrm{ch}}^{rot} = \omega L_{\mathrm{ch}} << v_{\infty}$$

Resolutions used for the sweep polar simulation

	Walls (m)	Wake (m)	Far Field (m)
Sweep Resolution Coarse	0.01	0.04	1.28
Sweep Resolution Fine	0.005	0.02	1.28

Polar Sweep

Sweep from the linear part of the polar to the stall region

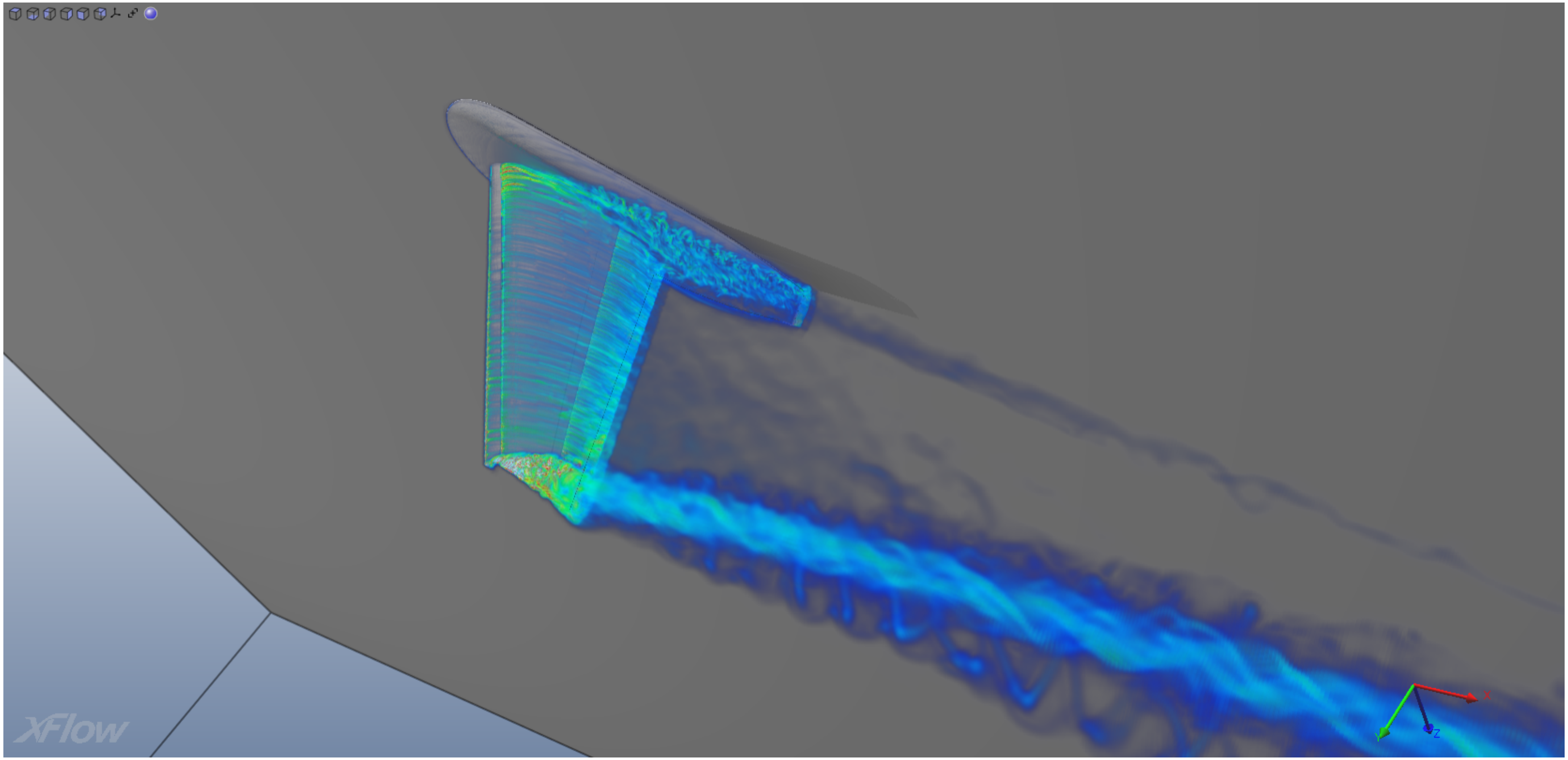

Polar Sweep

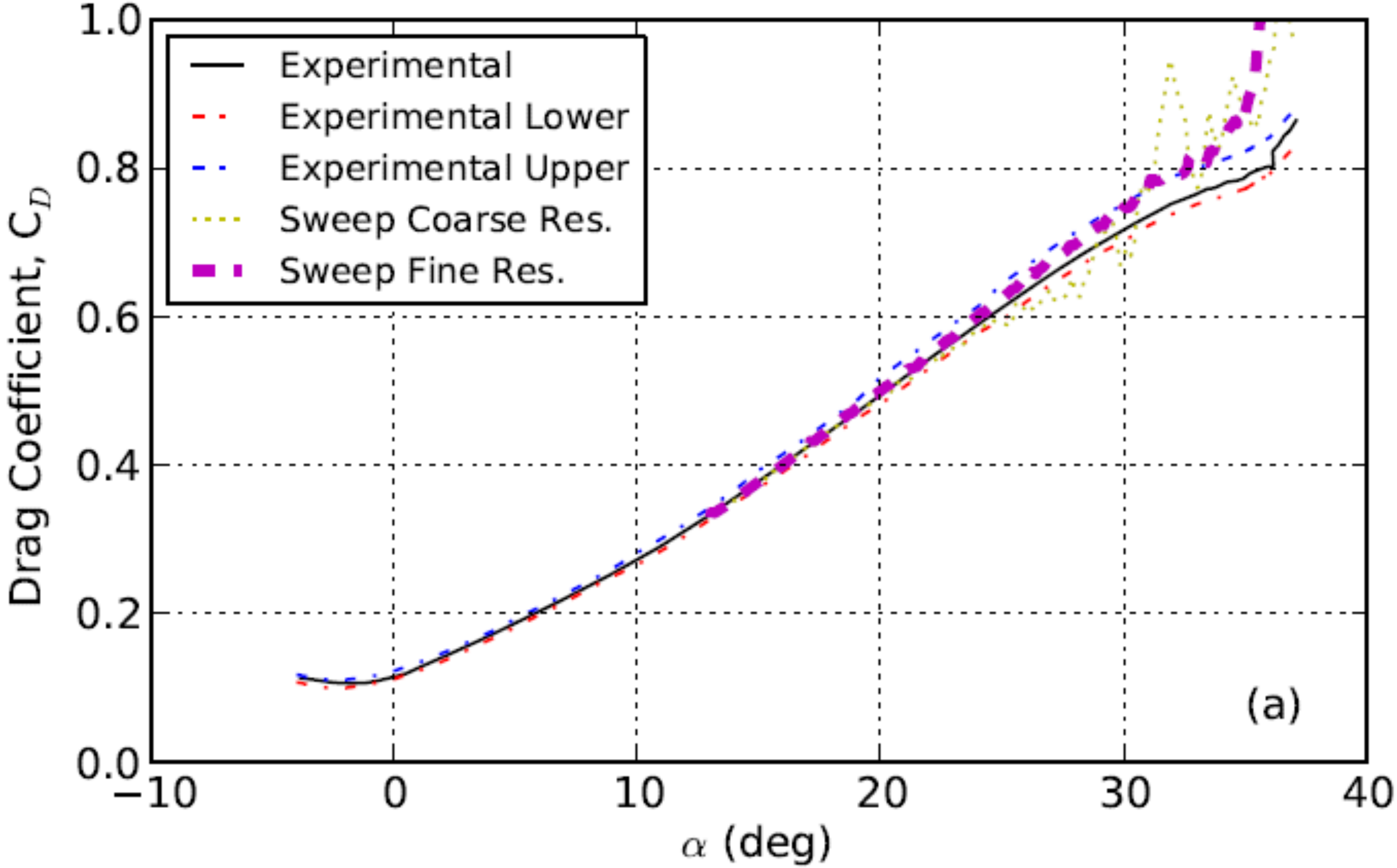

Experimental
Experimental Lower
Experimental Upper
Sweep Coarse Res.
Sweep Fine Res.
Drag Coefficient, C_D
α (deg)
(a)
1.0
0.8
0.6
0.4
0.2
0.0
−10
0
10
20
30
40

Polar Sweep

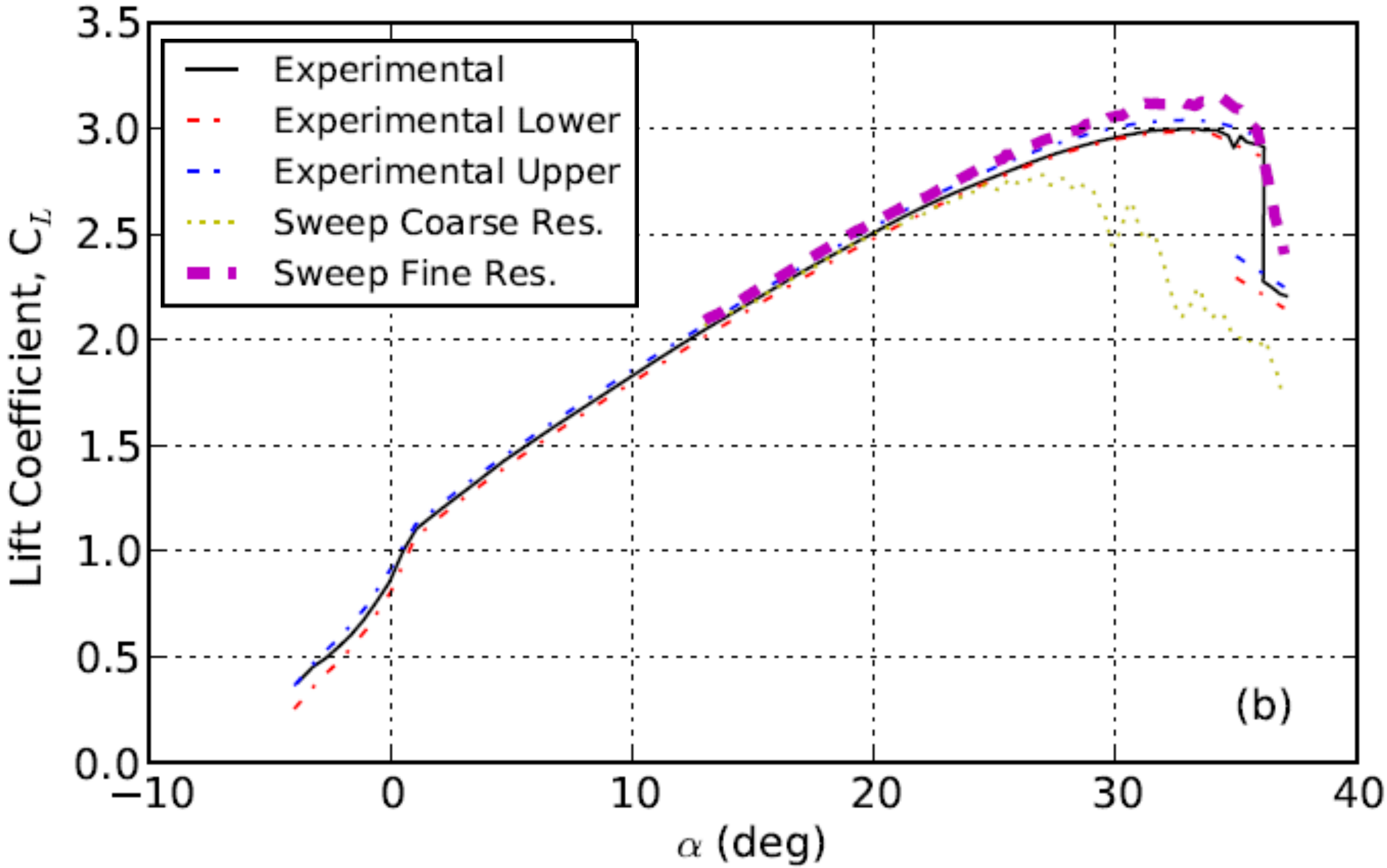

Experimental
Experimental Lower
Experimental Upper
Sweep Coarse Res.
Sweep Fine Res.
(b)
Lift Coefficient, C_L
α (deg)
3.5
3.0
2.5
2.0
1.5
1.0
0.5
0.0
−10
0
10
20
30
40

Polar Sweep

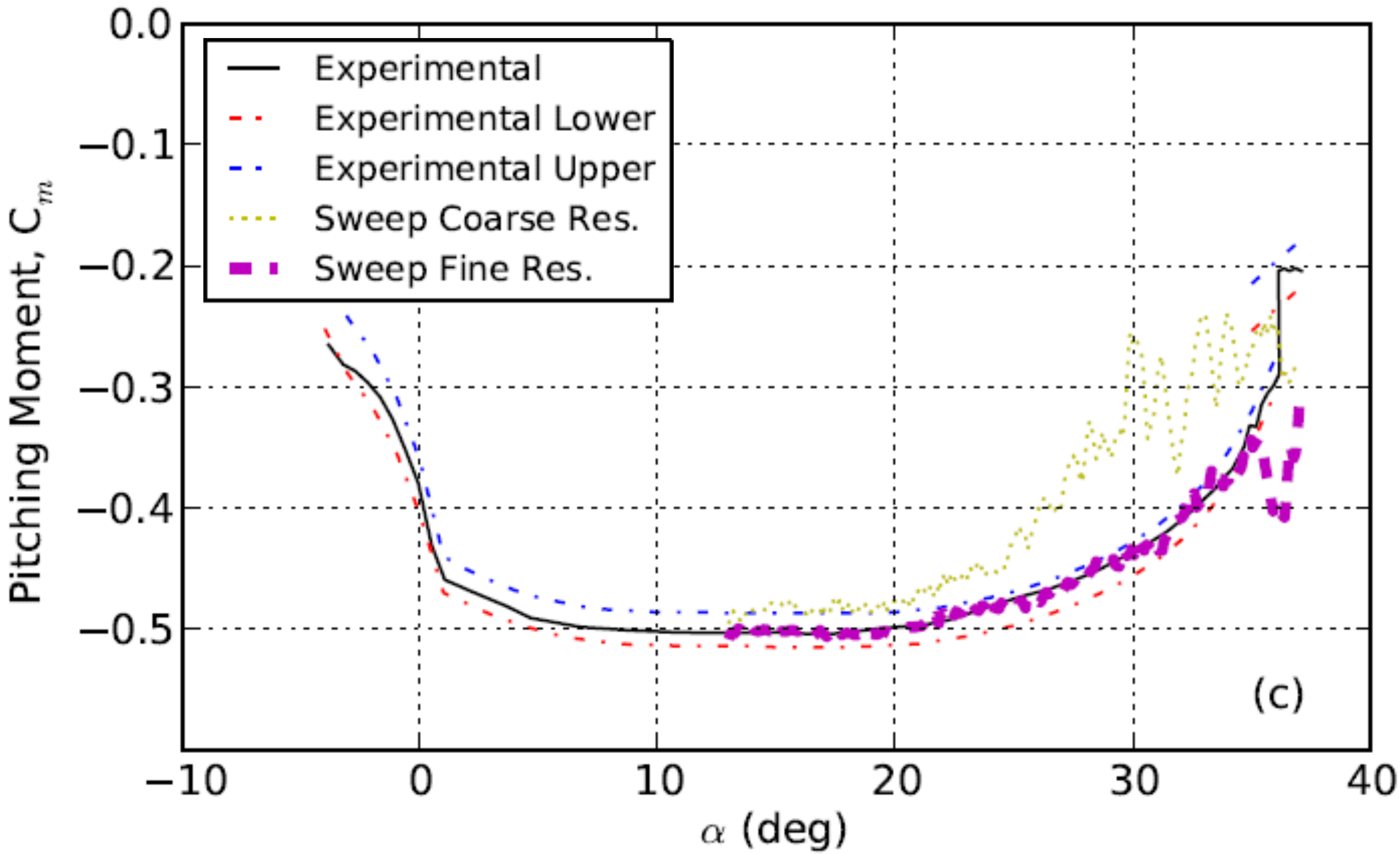

Experimental
Experimental Lower
Experimental Upper
Sweep Coarse Res.
Sweep Fine Res.
Pitching Moment, C_m
α (deg)
0.0
−0.1
−0.2
−0.3
−0.4
−0.5
−10
0
10
20
30
40
(c)

Outline

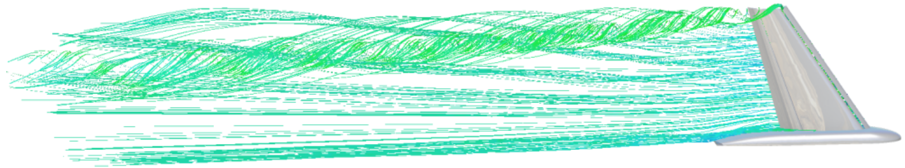

- Introduction
- Numerical Methodology
- 1st High Lift Prediction Workshop Results
- Polar Sweep
- **Stowing and Un-Stowing**
- Summary

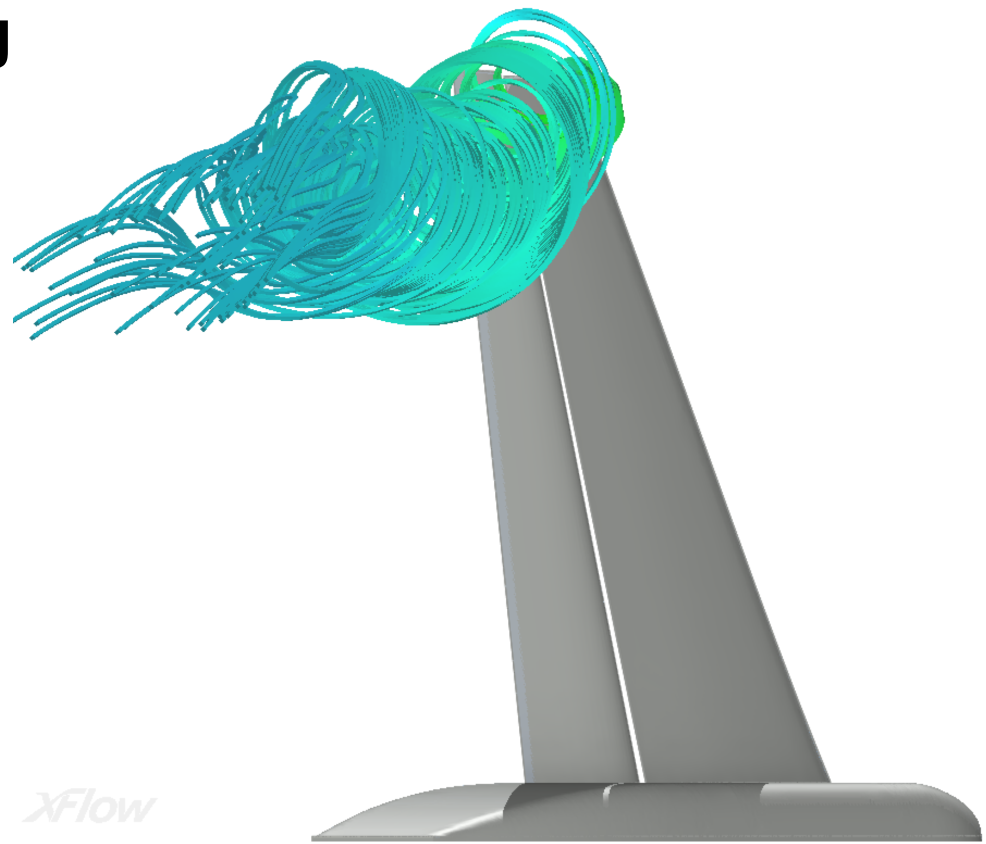

Stowing and Un-Stowing

The geometry has been separated into different components for the analysis of the stowing and un-stowing transitions of the flap and the slat

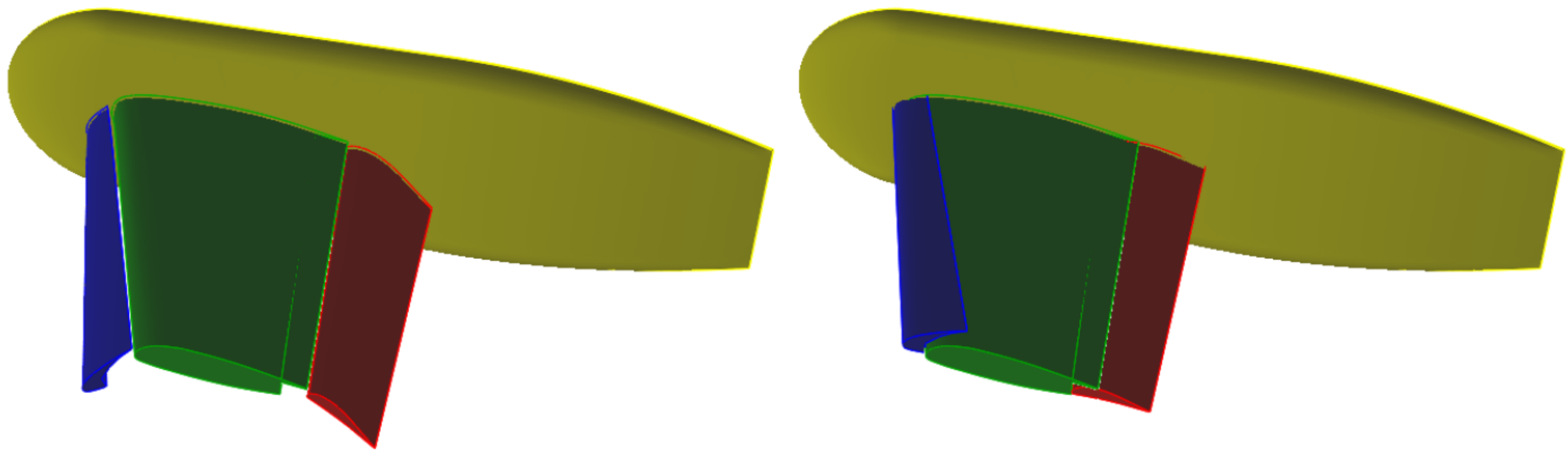

Un-stowed (left) and stowed (right) configurations

Stowing and Un-Stowing

Two different transformation laws have been analyzed

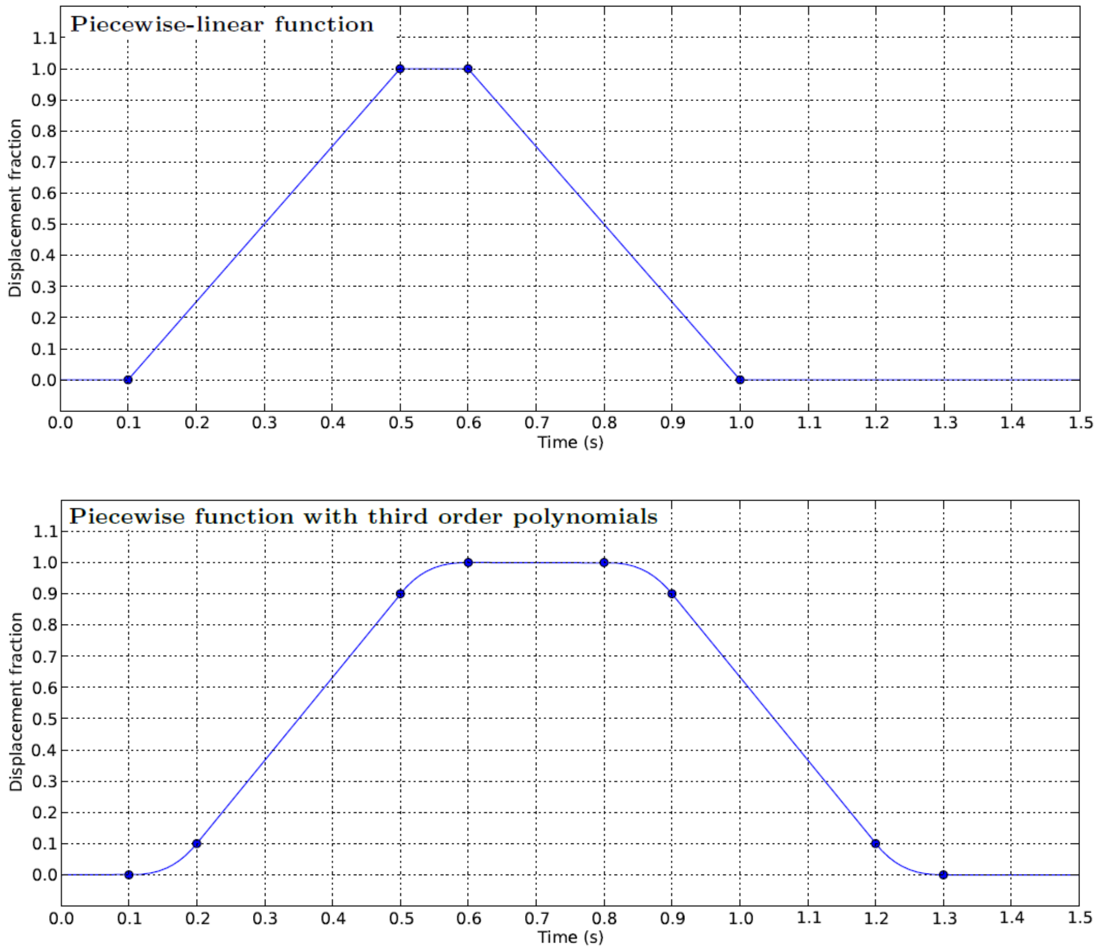

Stowing and Un-Stowing

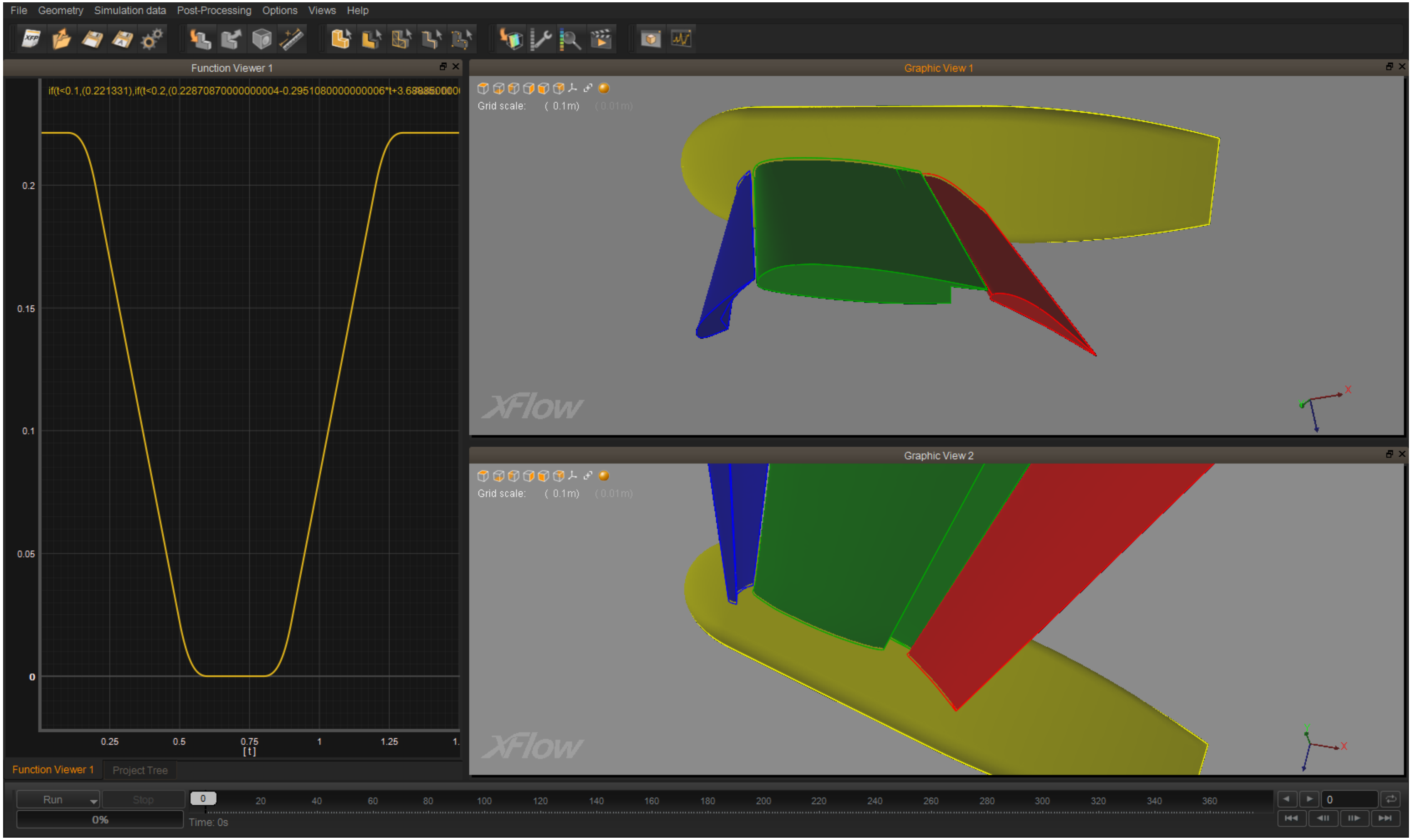

Stowing and Un-Stowing

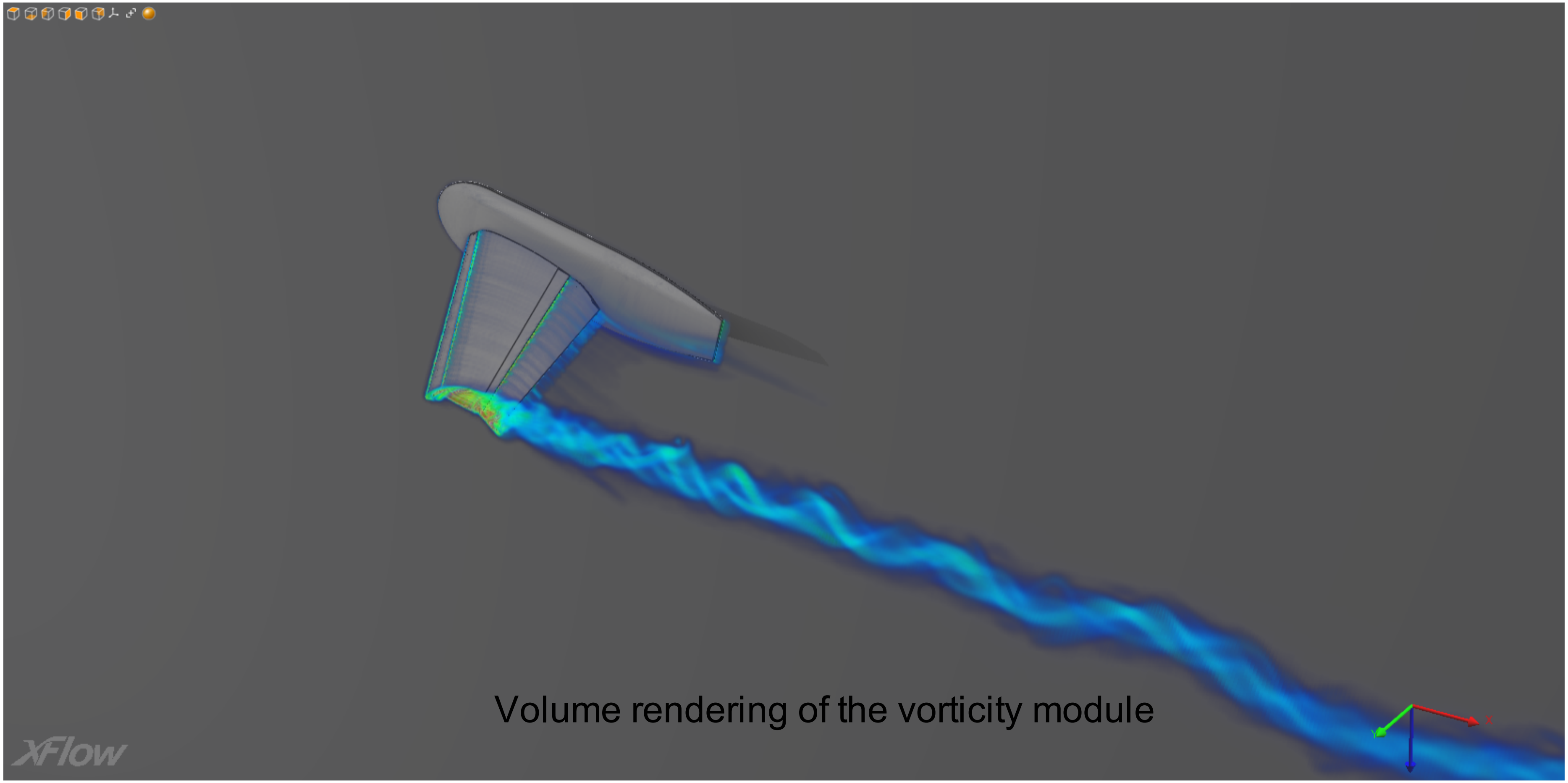

Stowing and Un-Stowing

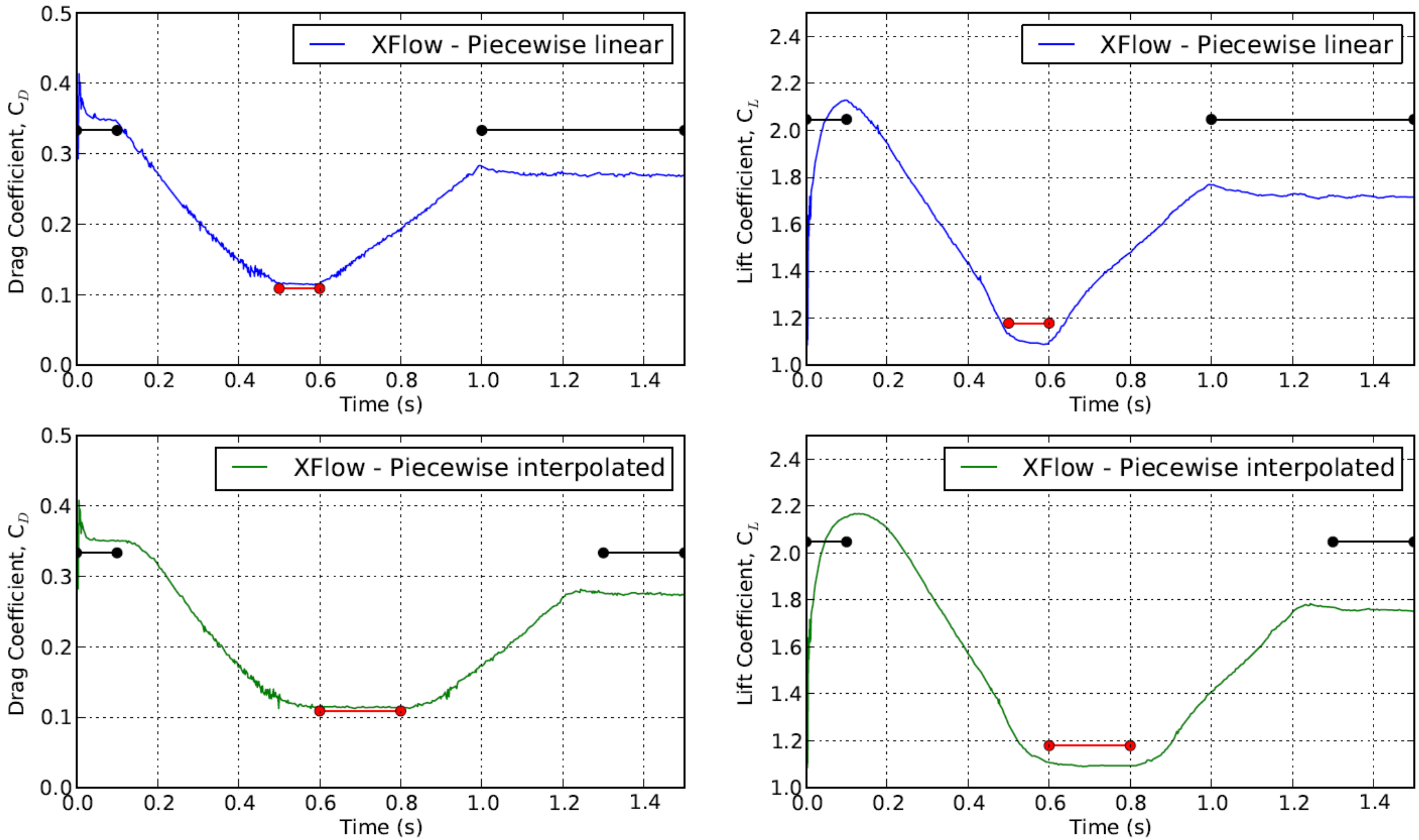

Summary

- XFlow has been proved a reliable tool for traditional and advanced aerodynamic problems involving presence of moving parts
- Results for the 1st HLPWF in good agreement with experimental data
- Successful polar sweep simulation
- Proof of concept simulation for the stowing and un-stowing maneuvers shows interesting results

Advanced Aerodynamic Analysis of the NASA High-Lift Trap Wing with a Moving Flap Configuration

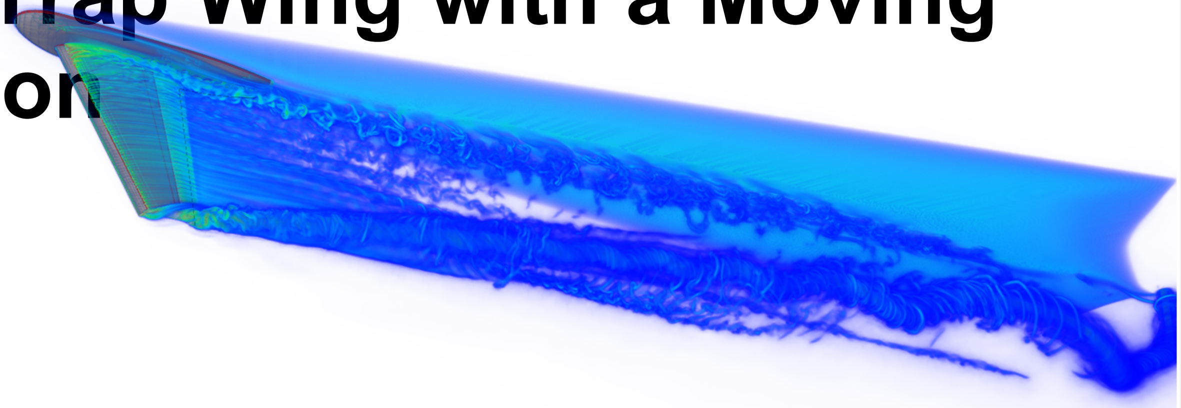

David M. Holman